2026 IEEE International Conference on Pervasive Computing and Communications Workshops and other Affiliated Events (PerCom Workshops) | 979-8-3315-7615-8/26/$31.00 ©2026 IEEE | DOI: 10.1109/PerComWorkshops68308.2026.11585202

AoI Optimization in 5G NR-V2X Sidelink through Propagation-Aware Dynamic Congestion Control

Ryo Iwaki *, Alexey Rolich†, Jin Nakazato ‡, Mert Yildiz †, Manabu Tsukada *, Andrea Baiocchi†
*The University of Tokyo, Japan
†University of Rome Sapienza, Italy
‡Tokyo University of Science, Japan
iwaki-ryo519@g.ecc.u-tokyo.ac.jp alexey.rolich@uniroma1.it
jin.nakazato@ieee.org mert.yildiz@uniroma1.it
mtsukada@g.ecc.u-tokyo.ac.jp andrea.baiocchi@uniroma1.it

***Abstract*—Maintaining low Age of Information (AoI) is essential for connected and autonomous vehicles, yet the Semi-Persistent Scheduling (SPS) procedure standardized for 5G NR-V2X sidelink employs a fixed sensing window that cannot adapt to changes in traffic load or vehicle density. This limitation increases resource-selection conflicts and degrades the timeliness required for cooperative perception and cooperative driving. This paper introduces a lightweight, fully distributed congestion-control mechanism that incorporates real-time congestion information into the SPS sensing process. By deriving statistics from neighboring transmission periodicity, the method dynamically adjusts the sensing-window span to reduce collisions and prevent excessive channel occupation. The approach is evaluated in a system-level framework combining microscopic mobility with a detailed wireless channel and SPS access model. Across diverse densities, mobility conditions, and communication ranges, the adaptive sensing-window mechanism consistently improves both mean and tail AoI and enhances the stability of the Resource Reservation Interval. It achieves substantial reductions in information staleness, including significant gains for short-range, safety-critical exchanges. Because it solely refines the sensing-window computation without modifying SPS signaling, the method offers a practical and readily deployable enhancement to NR-V2X Mode 2 congestion control.**

I. Introduction

Connected and Autonomous Vehicles (CAVs) require reliable and timely information exchange to support safe and efficient automated driving. Vehicle-to-Everything (V2X) communication enables real-time coordination among vehicles and infrastructure [1], [2], and large-scale field trials have demonstrated its essential role in next-generation transportation systems [3]. To meet stringent latency and reliability demands, 3GPP introduced 5G New Radio (NR)-V2X [4], which supports both infrastructure-assisted and decentralized resource allocation. In environments with limited network coverage or rapidly changing topology, Sidelink (SL) Mode 2 is the primary operating mode: vehicles autonomously select resources using sensing-based Semi-Persistent Scheduling (SPS) [5].

Beyond basic safety, 5G NR-V2X is designed to support advanced cooperative applications such as cooperative awareness, collective perception, and cooperative maneuvering [6]. By enabling vehicles to share sensor-derived information over the SL interface introduced in Release 16, NR-V2X extends perception beyond the Line-of-Sight (LOS) limitations of local sensors including LiDAR and Radar. This capability is essential for enhanced situational awareness in safety-critical scenarios.

NR-V2X defines two operational modes for SL communication [5]. In Mode 1, the gNodeB centrally schedules resources, which requires continuous network coverage. In contrast, Mode 2 allows vehicles to autonomously select resources using sensing-based SPS. Communication proceeds over resource chunks called Sub-Channel (SC). A vehicle selects the SCs it needs among those perceived as idle, based on channel sensing and Sidelink Control Information (SCI). The vehicle reuses the same SC for a randomized number of successive transmission opportunities. The key SPS parameters governing the persistence of SCs use are the Resource Reservation Interval (RRI), the Reselection Counter (RC), and the persistence probability [6].

Although SPS reduces control overhead and scales naturally with network density, its distributed nature makes it increasingly susceptible to collisions at high vehicle densities. The sensing window determines the candidate resource set, and suboptimal configurations increase collision probability and degrade the Age of Information (AoI) [7]–[10]. AoI quantifies the freshness of status updates and is critical for cooperative awareness, collective perception, and cooperative maneuvering [11]. Ensuring low AoI is therefore fundamental to advanced CAV safety-related applications.

Congestion control for NR-V2X Mode 2 has received considerable attention. Since decentralized SPS lacks a central scheduler, 3GPP provides congestion indicators such as Channel Busy Ratio (CBR) and collision risk, but no prescribed control algorithm. This has led to efforts adapting the ETSI Distributed Congestion Control (DCC) framework to cellular V2X. Mansouri *et al.* [12] and Toghi *et al.* [13] showed that direct application of DCC to LTE-V2X Mode 4 can worsen performance due to adverse interactions with SPS. Choi *et al.* [14] proposed a Deep Reinforcement Learning (DRL)-based algorithm that adjusts transmission rate and channel utilization, achieving improved Packet Reception Ratio (PRR) while maintaining target CBR.

Recent analytical and algorithmic studies broaden the de-

Authorized licensed use limited to: Universita degli Studi di Roma La Sapienza. Downloaded on October 27,2026 at 15:13:50 UTC from IEEE Xplore. Restrictions apply.

979-8-3315-7615-8/26/$31.00 ©2026 IEEE

sign space for decentralized congestion control in NR-V2X Mode 2. Fu *et al.* [15] developed a stochastic-geometry model of Cooperative Awareness Message (CAM) broadcast under Mode 2 SPS, derived closed-form expressions for collision probability, PRR, CBR, throughput, and proposed a decentralized rate-adaptation scheme. Sarkis *et al.* [16] evaluated Release 16 distributed congestion-control mechanisms and identified robust parameter configurations using hybrid resource-consumption control. Power-control-based congestion control is investigated in [17], which proposed an Signal-to-Interference-plus-Noise Ratio (SINR)-driven open-loop power-control strategy achieving notable PRR gains. Hybrid optimization across message rate, SC bandwidth, and Modulation and Coding Scheme (MCS) was explored in [18], while joint rate–power control in LTE-V2X was addressed in [19] via multi-agent DRL. Graph-based multi-agent learning for generic V2X congestion control was proposed in [20].

Despite substantial progress, most existing approaches focus on maintaining acceptable CBR or maximizing throughput, with limited integration of application-level timeliness requirements. These methods typically optimize only a subset of parameters (rate, power, MCS, or resource allocation) and often neglect the impact of congestion-control decisions on AoI.

AoI has emerged as a critical performance metric in V2X systems, capturing the freshness of situational information at the receiving vehicle [21], [22]. Stale information can degrade cooperative perception accuracy and negatively impact automated driving performance [23]. Only a small number of studies explicitly consider AoI in NR-V2X Mode 2 congestion control [24]–[26]. Saad *et al.* [25] propose a DRL-based controller optimizing medium-access parameters with explicit AoI consideration, achieving gains in PRR, average AoI, throughput, and CBR. Dayal *et al.* [26] propose channel-aware and AoI-aware RRI selection policies, showing that combining these with SPS improves performance under diverse conditions.

Our paper addresses this gap by extending the AoI-driven congestion-control framework proposed in [27]. The prior work introduces an adaptive, fully distributed NR-V2X Mode 2 algorithm that jointly adjusts the SPS persistence probability and the RRI to minimize average AoI. Its adaptation strategy operates along two dimensions: data-rate regulation through RRI selection and long-term channel-occupancy control through persistence probability, without incorporating power or MCS adaptation.

The contributions of this paper are summarized as follows:

- We refine the adaptation mechanism by introducing a dynamic sensing-window adjustment strategy that ensures stable and efficient operation across a broad range of vehicle densities.
- We extend the evaluation of AoI-aware, persistence-driven congestion control by incorporating more realistic mobility and wireless-channel models. In particular, we replace the simplified assumptions in [27] with a realistic Simulation of Urban Mobility (SUMO) [28]-based mobility and a propagation model that captures both deterministic distance-dependent path loss and stochastic fading.
- We provide an extensive performance assessment. The results show consistent improvements across diverse conditions and robust performance of the distributed algorithm.

As for the remainder of the paper, the proposed propagation-aware dynamic congestion-control mechanism and the associated adaptive sensing-window control are detailed in Section II. The simulation setup, environment, and evaluation scenarios are described in Section III. Numerical results and performance analysis are presented in Section IV. Concluding remarks are provided in Section V.

II. Adaptive Window-Size Control

To overcome the limitations of the idealized assumptions in prior work [27] and improve SPS congestion control under realistic conditions, this section details our proposed method.

Our core contribution is a new dynamic control of the sensing window in SPS to mitigate resource-selection conflicts. We first outline the challenges of the standard SPS and then detail the design of the proposed method.

In the 3GPP standard SPS, a vehicle requiring resources observes other vehicles' transmissions within a sensing window, compiles a candidate list of available resources, and then selects one SC at random among those deemed to be available. The selected SC is reused with time period RRI for a certain number of times [29], [30].

The standard prescribes a fixed sensing window of about 1 s, independent of the selected RRI. The sensing window size, measured in time slots, is given by

$$W_{std} = \frac{T_{sw}}{T_s}, \quad T_{sw} = 1 \text{ s}. \tag{1}$$

where T_{sw} is the duration of the sensing window and T_s is the time slot size.

Since this window length remains constant even when the environment changes, it is insensitive to actual network congestion. In particular, when the vehicle density increases and vehicles choose shorter RRI values, W_{std} can become excessively large relative to transmission periodicity, creating excessive resource contention and degrading AoI.

To address this issue, we introduce the spatial average of RRI observed from neighboring vehicles (RRI_{avg}) as an indicator that directly reflects current congestion, and dynamically compute a new window size W_{new} as

$$W_{new} = \max\left(W_{min}, \beta \cdot \frac{RRI_{avg}}{T_s \cdot n_s}\right) \tag{2}$$

where n_s is the number of SCs in a time slot. This equation is based on the following considerations:

- **Use of RRI_{avg}:** RRI_{avg} directly reflects the average transmission periodicity chosen by nearby vehicles and therefore the present network load. Incorporating it allows the window to adapt dynamically to the actual congestion and maintain the candidate range.

Authorized licensed use limited to: Universita degli Studi di Roma La Sapienza. Downloaded on October 27,2026 at 15:13:50 UTC from IEEE Xplore. Restrictions apply.

- **Lower bound W_{min}:** Using $\max(\cdot)$ guarantees that the window never falls below a minimum value W_{min} derived from the smallest allowed RRI, preserving resource-selection opportunities and ensuring stability even under unexpected conditions.
- **Role of β:** The tuning coefficient β ($0 < \beta \leq 1$) adjusts the sensitivity of the window size to variations in RRI_{avg}, enabling scenario-dependent optimization and allowing the window to shrink below the 3GPP baseline, when the observed RRIs are short.

The proposed adaptive window-size control is integrated into a realistic SUMO-based mobility and propagation model within the V2X simulator [31]. Its core operations – averaging the observed RRIs and computing the dynamic window – are $O(N)$ in the number of neighboring vehicles and require minimal changes to the existing SPS resource selection logic.

The distributed congestion-control procedure operates as follows. The algorithm first collects the RRIs advertised or inferred from neighboring vehicles. When observations are available, their spatial average is computed; otherwise, a conservative maximum value is adopted. Using this estimate, the sensing-window size is updated according to the adaptive rule, ensuring responsiveness to local congestion conditions while preventing excessive window reduction. The resulting window is then applied within the RRI adaptation mechanism [27] to update the node's transmission periodicity RRI_{node}. After the RRI has been adapted, the node performs sensing over the computed window to identify feasible resources. If suitable candidate SCs are found, the node selects one at random and reserves it; otherwise, it triggers a congestion-handling routine. This process enables distributed and adaptive resource selection, guided by local traffic load and observed transmission behavior. Algorithm 1 presents the resulting resource-selection and reservation procedure with the proposed AoI-aware, persistence-driven congestion control and adaptive sensing window.

Algorithm 1 SPS resource selection using AoI-aware and persistence-driven congestion control with adaptive window-size control

Input: RRI_{max}, W_{min}, β, T_s, n_s, RRI_{node}
Output: Selected resource $r_{selected}$

// Step 1: Obtain the list of RRIs observed from neighbors
$observed_RRIs \leftarrow getObservedRRIsFromNeighbors()$

// Step 2: Compute average RRI
if $observed_RRIs$ is not empty **then**
    $RRI_{avg} \leftarrow calcMovingAverage(observed_RRIs)$
else
    $RRI_{avg} \leftarrow RRI_{max}$ // Use the maximum if no observation

// Step 3: Dynamic window computation (proposed)
$W_{new} \leftarrow \max(W_{min}, \beta \cdot (RRI_{avg}/T_s)/n_s)$

// Step 4: RRI adaptation using algorithm proposed in [27] with W_{new}
$RRI_{node} \leftarrow adaptRRI(W_{new}, RRI_{node}, RRI_{avg})$

// Step 5: Perform sensing
$sensing_window \leftarrow W_{new}$
$available_resources \leftarrow performSensing(sensing_window)$

// Step 6: Select and reserve a resource
if $available_resources$ is not empty **then**
    $r_{selected} \leftarrow selectRandomResource(available_resources)$
    $reserveResource(r_{selected})$
else
    // Handling when no resource is available (e.g., congestion)
    $handleCongestion()$
return $r_{selected}$

III. Simulation setup

This section describes the simulation environment, scenarios, system parameters, and evaluation metrics used to assess the proposed adaptive sensing-window control. The setup integrates realistic microscopic mobility with a detailed V2X communication model, enabling controlled and reproducible experimentation across diverse traffic densities and mobility conditions.

A. Simulation Environment

We develop a simulation framework that reproduces realistic vehicular communication conditions through two tightly integrated components: a microscopic traffic-flow simulator and a system-level V2X communication simulator. Vehicle mobility is generated using SUMO, which provides per-timestep trajectories including positions, speeds, and accelerations for both urban and highway scenarios. Mobility traces serve as input to the propagation model within the V2X simulator that performs the communication-layer evaluation. The V2X simulator models the physical layer using a propagation pipeline that replaces collision abstractions with channel-based decoding. Path loss is computed via a log-distance model with LOS/Non-Line-of-Sight (NLOS) switching as a function of inter-vehicle distance, and includes Gaussian shadowing. SINR-based decoding is performed, accounting for interference from all active transmitters. PHY-layer packet outcomes are forwarded to the MAC layer, where the SPS mechanism carries out sensing, resource selection, and reservation. The proposed adaptive sensing-window control is implemented within this MAC-layer module.

To maintain cross-layer consistency, identical random seeds are used for PHY and MAC operations, and per-packet logs map SUMO vehicle identifiers to communication events. This prevents double-counting of collisions and simplifies validation of SPS decisions. All propagation and SPS parameters are configurable, ensuring reproducible experiments and con-

Authorized licensed use limited to: Universita degli Studi di Roma La Sapienza. Downloaded on October 27,2026 at 15:13:50 UTC from IEEE Xplore. Restrictions apply.

TABLE I
SIMULATION PARAMETERS

Category	Parameter	Value
RF settings	Carrier frequency	5.9 GHz
	Bandwidth	10 MHz
	Transmit power	23 dBm
	Receiver sensitivity	-95 dBm
Propagation model	Path loss model	Log-distance with LOS/NLOS switch
	Shadowing	6 dB (Gaussian)
SPS settings	RRI range	[1, 1000] ms
	Initial RRI	100 ms
	Persistence probability	0.8
Proposed method	Tuning factor β	1.0
	Minimum window	5 slots

sistent comparison across baseline and proposed methods.

B. Evaluation Scenarios and System Parameters

Two representative vehicular environments are considered to evaluate the proposed method, covering density-driven and mobility-driven dynamics in NR-V2X Mode 2. These scenarios span a wide operating range of SPS contention, Doppler-induced channel variation, and topology evolution:

- Urban scenario (5 km straight road). This configuration models medium-scale urban traffic with progressively increasing density. We consider three vehicle populations, $N = 25, 100, 198$, representing sparse, moderate, and dense traffic conditions. Vehicles travel at an average speed of approximately 50 km/h. This scenario is used to quantify the sensitivity of the method to density-induced contention and packet-collision effects.
- Highway scenario (5 km straight road). A higher-mobility environment is modeled with $N = 66$ vehicles moving at an average speed of approximately 80 km/h. The scenario captures rapid topological changes and stronger Doppler effects, providing an assessment of robustness under fast mobility with lower traffic density.

Table I summarizes the simulation parameters. Radio-frequency, propagation, and SPS configurations follow 3GPP NR-V2X specifications to maintain comparability with prior work [29]. Propagation settings adopt a log-distance path-loss model with LOS/NLOS switching [32] and Gaussian shadowing. SPS parameters and method-specific tuning factors are included for reproducibility. The detailed symbol allocation is specified in the standard and summarized for the considered simulation model in [33].

Unless otherwise stated, the results are compared with the baseline that uses the fixed 3GPP-compliant sensing window defined in [29]. Each data point averages 1000 s of simulation over multiple random seeds; we omit confidence intervals for brevity, but the relative variations across seeds were consistently below 5 %.

C. Evaluation Metric

We evaluate the evolution of the RRI and the resulting time-averaged AoI during operation of the proposed algorithm. In addition, the 95th percentile AoI is reported to quantify the tail of the AoI distribution, highlighting worst-performing links that are particularly relevant for safety-critical applications. In all simulations, the initial RRI is randomly assigned, and the value of the RC is dynamically updated according to the NR-V2X standard. A distance-limited evaluation is also performed to examine performance within a communication range of 200 m. This directly targets short-range links relevant to safety applications, enabling assessment of information freshness for collision avoidance and other time-critical use cases.

For each transmitter–receiver link (i, j) in the evaluation link set $\mathcal{L}$, we compute the time-averaged AoI over the simulation duration T as

$$\langle A_{i,j} \rangle(T) = \frac{1}{T} \int_0^T \mathrm{AoI}_{i,j}(\tau)\, d\tau. \tag{3}$$

The overall mean AoI is the spatial average across links:

$$\bar{A} = \frac{1}{|\mathcal{L}|} \sum_{(i,j)\in\mathcal{L}} \langle A_{i,j} \rangle(T). \tag{4}$$

The 95th percentile AoI is computed from the distribution of $\{\langle A_{i,j} \rangle(T)\}$ over $\mathcal{L}$. For the distance-limited evaluation, $\mathcal{L}$ is restricted to links within 200 m.

IV. PERFORMANCE EVALUATION

This section presents a detailed performance assessment of the proposed adaptive sensing-window control across a wide range of vehicular densities and mobility conditions. The analysis focuses on mean and tail AoI, the evolution and variability of the RRI, and the method's impact on short-range communication relevant to safety-critical applications. Results are reported for sparse, medium, and dense urban traffic, as well as high-speed highway scenarios, enabling a comprehensive examination of the underlying mechanisms driving the observed improvements.

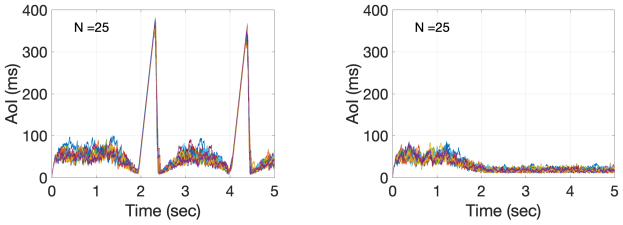
A. AoI analysis

1) Improvement in sparse traffic ($N = 25$) and underlying mechanisms: The largest gains appear in sparse traffic. As shown in Fig. 1, mean AoI drops from 66.2 ms to 27.5 ms, a 58.4 % reduction. The fixed window in conventional SPS is overly large relative to the available resources in low density, leaving many usable resources idle. By dynamically tailoring the window using the observed average RRI, the proposed method removes this inefficiency.

Notably, the 95th percentile AoI improves from 266.9 ms to 56.5 ms (78.8 %). This indicates that the adaptive window control effectively enables the following:

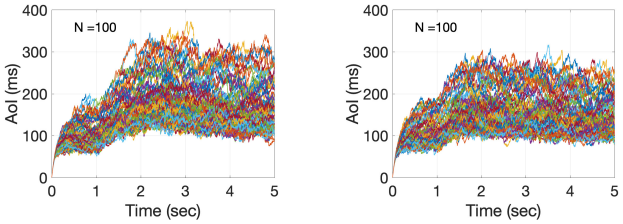
1) **Collision reduction:** Dynamic window tuning suppresses unnecessary collisions.
2) **Suppression of extreme degradation:** The large improvement in the 95th percentile curbs worst-case performance.
3) **Stability gain:** RRI standard deviation improves from 39.8 ms to 36.3 ms (8.8 %).

Authorized licensed use limited to: Universita degli Studi di Roma La Sapienza. Downloaded on October 27,2026 at 15:13:50 UTC from IEEE Xplore. Restrictions apply.



(a) Without proposal (b) With proposal

Fig. 1. AoI over time in the sparse scenario ($N = 25$).



(a) Without proposal (b) With proposal

Fig. 2. AoI over time in the medium-density scenario ($N = 100$).

The mean RRI also shortens from 57.6 ms to 47.2 ms, showing that surplus resources are utilized more evenly even in sparse conditions.

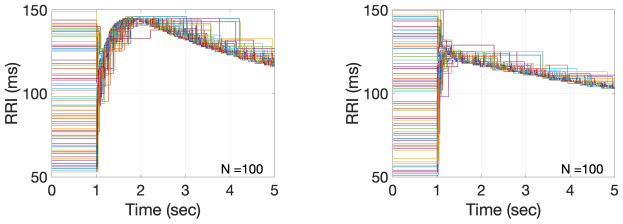
2) Stability-oriented gains in medium density ($N = 100$): In medium density, mean AoI improves by 7.7 % (143.1 ms to 132.0 ms) as shown in Fig. 2. Although the margin is smaller than that in sparse traffic, the following gains are significant:

- 95th percentile AoI: 260.6 ms to 235.1 ms (9.8 % improvement).
- RRI standard deviation: 21.4 ms to 14.7 ms (31.1 % improvement).
- Mean RRI: 124.4 ms to 111.5 ms (10.4 % reduction).

The 31.1 % reduction in the RRI variance indicates markedly improved predictability and stability, suggesting that the proposed method prioritizes stability over raw performance gain in medium density.

3) Performance in dense traffic ($N = 198$): Even under severe congestion, the proposed method offers benefits. Fig. 4 shows:

- Mean AoI: 353.6 ms to 328.6 ms (7.1 %).

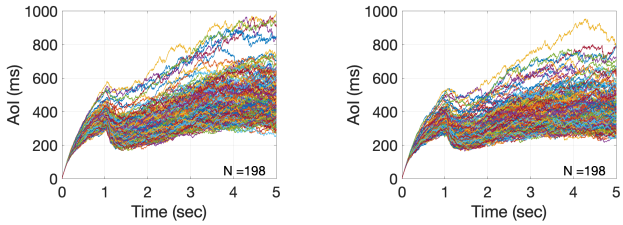


(a) Without proposal (b) With proposal

Fig. 3. RRI over time in the medium-density scenario ($N = 100$).

TABLE II
RRI STATISTICS ACROSS ALL SCENARIOS

Scenario	RRI std. dev. (ms)		Mean RRI (ms)	
	Before	After	Before	After
$N = 25$	39.8	36.3	57.6	47.2
$N = 100$	21.4	14.7	124.4	111.5
$N = 198$	55.3	39.5	193.1	169.2
Highway	19.1	16.6	89.9	81.5



(a) Without proposal (b) With proposal

Fig. 4. AoI over time in the dense scenario ($N = 198$).

- 95th percentile AoI: 593.6 ms to 531.9 ms (10.4 %).
- RRI standard deviation: 55.3 ms to 39.5 ms (28.6 %).
- Mean RRI: 193.1 ms to 169.2 ms (12.4 %).

This demonstrates that the proposed control provides a consistent improvement, even when spectrum scarcity dominates.

4) Robustness on highways: Despite frequent topology changes due to high speed, the method remains effective, as shown in Fig. 5.

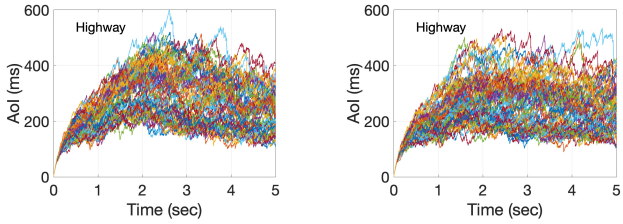
- Mean AoI: 255.3 ms to 238.3 ms (6.6 %).
- 95th percentile AoI: 421.0 ms to 392.9 ms (6.7 %).
- RRI standard deviation: 19.1 ms to 16.6 ms (13.0 %).
- Mean RRI: 89.9 ms to 81.5 ms (9.4 %).

B. Advantages in Short-Range Communication

Limiting evaluation to 200 m highlights the advantages of the proposed method by excluding failures for distant vehicles and focusing on information relevant to immediate safety.

Short-range communication within 200 m is vital for collision avoidance and related safety applications [34]. The following results show that the proposed method directly enhances safety:

- $N = 25$: Mean AoI 29.4 ms $\rightarrow$ 10.9 ms (62.9 %).



(a) Without proposal (b) With proposal

Fig. 5. AoI over time in the highway scenario.

Authorized licensed use limited to: Universita degli Studi di Roma La Sapienza. Downloaded on October 27,2026 at 15:13:50 UTC from IEEE Xplore. Restrictions apply.

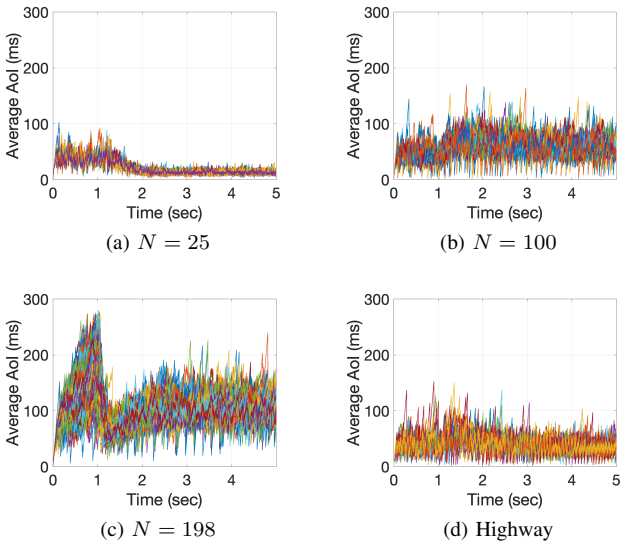


Fig. 6. AoI performance within 200 m after applying the proposed method.

TABLE III
AOI IMPROVEMENTS WITHIN 200 M

Scenario	Before (ms)	After (ms)	Improvement (%)
$N = 25$	29.4	10.9	62.9
$N = 100$	31.3	28.4	9.3
$N = 198$	57.0	51.9	8.9
Highway	22.0	20.4	7.3

- $N = 100$: Mean AoI 31.3 ms $\rightarrow$ 28.4 ms (9.3 %).
- $N = 198$: Mean AoI 57.0 ms $\rightarrow$ 51.9 ms (8.9 %).
- Highway: Mean AoI 22.0 ms $\rightarrow$ 20.4 ms (7.3 %).

The 62.9 % improvement in sparse traffic exceeds the 58.4 % gain over the full range, underscoring the method's effectiveness for close-range exchanges. Fig. 6 and Table III detail these improvements.

V. CONCLUSION

We proposed an adaptive sensing-window control mechanism for 5G NR-V2X SL congestion control and demonstrated that it significantly improves information freshness under realistic vehicular mobility and interference conditions. The evaluation shows consistent gains in both mean and tail AoI, reduced variability in RRI, and substantial benefits for short-range safety-relevant links.

TABLE IV
AOI IMPROVEMENTS ACROSS ALL SCENARIOS

Scenario	AoI improvement (%)		RRI std. dev.
	Mean AoI	95th percentile AoI	Improvement (%)
$N = 25$	58.4	78.8	8.8
$N = 100$	7.7	9.8	31.1
$N = 198$	7.1	10.4	28.6
Highway	6.6	6.7	13.0

- Mean AoI reduced by 58.4 % and 95th percentile AoI reduced by 78.8 % in sparse traffic ($N = 25$).
- RRI variability lowered by 8.8 %–31.1 % across all scenarios.
- Up to 62.9 % AoI reduction within 200 m for safety-critical short-range links.

These results indicate that the proposed method provides a practical and effective mechanism for improving AoI in NR-V2X systems, enhancing timeliness especially where safety applications impose strict freshness requirements.

Our study is simulation-based and restricted to straight-road urban and highway settings, and the achievable improvement depends on traffic density and spectrum availability. In dense conditions, channel scarcity limits the attainable gains. The model also assumes perfect synchronization and full Physical sidelink shared channel (PSSCH) decodability; partial decoding could bias the estimated RRI_{avg} and merits further investigation.

Future work includes validation in real-world environments, extension to more complex road geometries, and integration with complementary DCC mechanisms such as adaptive power control. Additional directions include analyzing the responsiveness–stability tradeoff in computing RRI_{avg}, exploring switching among pre-tuned β profiles, and evaluating fairness under partial observations, including mechanisms such as candidate reseeding or fallback to W_{std}.

ACKNOWLEDGMENT

This research is supported in part by JST ASPIRE Grant Number JPMJAP2325. It is supported in part by JSPS KAKENHI under Grant 25K17605. It is partially funded by Sapienza University of Rome through the 2024 program "Progetti per Avvio alla Ricerca - Tipo 2", grant AR2241906D14C736, for the project "Enhancing Resource Allocation Mechanisms in 5G NR-V2X Sidelink Communications: Optimization and Performance Evaluation", and through grant RP123188F68315A5 for the project "Modeling and optimization of SL communications in Cellular V2X (C-V2X) 5G NR". It is also partially supported by the Ministry of University and Research of Italy under the PRIN program, project code 20223Y85JN, titled "LOREN - LOw-delay congestion control for REal-time applications over the iNternet" (CUP B53D23002200006).

REFERENCES

[1] C. Campolo, A. Molinaro, A. Iera, and F. Menichella, "5G Network Slicing for Vehicle-to-Everything Services," *IEEE Wireless Communications*, vol. 24, no. 6, pp. 38–45, 2017.

[2] Y. Asabe, E. Javanmardi, J. Nakazato, M. Tsukada, and H. Esaki, "Enhancing reliability in infrastructure-based collective perception: A dual-channel hybrid delivery approach with real-time monitoring," *IEEE Open Journal of Vehicular Technology*, vol. 5, pp. 1124–1138, 2024.

[3] V. Maglogiannis, D. Naudts, S. Hadiwardoyo, D. van den Akker, J. Marquez-Barja, and I. Moerman, "Experimental V2X evaluation for C-V2X and ITS-G5 technologies in a real-life highway environment," *IEEE Transactions on Network and Service Management*, vol. 19, no. 2, pp. 1521–1538, 2022.

Authorized licensed use limited to: Universita degli Studi di Roma La Sapienza. Downloaded on October 27,2026 at 15:13:50 UTC from IEEE Xplore. Restrictions apply.

[4] M. Harounabadi, D. M. Soleymani, S. Bhadauria, M. Leyh, and E. Roth-Mandutz, "V2X in 3GPP standardization: NR sidelink in release-16 and beyond," *IEEE Communications Standards Magazine*, vol. 5, no. 1, pp. 12–21, 2021.

[5] Z. Ali, S. Lagén, L. Giupponi, and R. Rouil, "3GPP NR V2X mode 2: overview, models and system-level evaluation," *IEEE Access*, vol. 9, pp. 89 554–89 579, 2021.

[6] M. H. C. Garcia, A. Molina-Galan, M. Boban, J. Gozalvez, B. Coll-Perales, T. Şahin, and A. Kousaridas, "A tutorial on 5G NR V2X communications," *IEEE Communications Surveys & Tutorials*, vol. 23, no. 3, pp. 1972–2026, 2021.

[7] A. Rolich, M. Yildiz, I. Turcanu, A. Vinel, and A. Baiocchi, "Rethinking Persistent Scheduling in 5G New Radio Vehicle-to-Everything Sidelink Communications," *IEEE Access*, vol. 13, pp. 164 065–164 083, 2025.

[8] ——, "On the Trade-off Between AoI Performance and Resource Reuse Efficiency in 5G NR V2X Sidelink," in *2025 IEEE Vehicular Networking Conference (VNC)*, 2025, pp. 1–8.

[9] A. Rolich, I. Turcanu, A. Vinel, and A. Baiocchi, "Understanding the impact of persistence and propagation on the Age of Information of broadcast traffic in 5G NR-V2X sidelink communications," *Computer Networks*, vol. 248, p. 110503, 2024.

[10] ——, "Impact of Persistence on the Age of Information in 5G NR-V2X Sidelink Communications," in *21st Mediterranean Communication and Computer Networking Conference (MedComNet)*, Ponza Island, Italy, Jun. 2023, pp. 15–24.

[11] S. Kaul, M. Gruteser, V. Rai, and J. Kenney, "Minimizing age of information in vehicular networks," in *8th Annual IEEE Communications Society Conference on Sensor, Mesh and Ad Hoc Communications and Networks*, 6 2011, pp. 350–358.

[12] A. Mansouri, V. Martinez, and J. Härri, "A first investigation of congestion control for LTE-V2X mode 4," in *15th Annual Conference on Wireless On-demand Network Systems and Services (WONS)*. IEEE, 2019, pp. 56–63.

[13] B. Toghi, M. Saifuddin, Y. P. Fallah, and M. O. Mughal, "Analysis of distributed congestion control in cellular vehicle-to-everything networks," in *IEEE 90th Vehicular Technology Conference (VTC2019-Fall)*. IEEE, 2019, pp. 1–7.

[14] J.-Y. Choi, H.-S. Jo, C. Mun, and J.-G. Yook, "Deep reinforcement learning-based distributed congestion control in cellular V2X networks," *IEEE Wireless Communications Letters*, vol. 10, no. 11, pp. 2582–2586, 2021.

[15] Q. Fu, J. Liu, J. Wang, and J. Kong, "Optimizing Throughput for NR V2X Message Delivery with Congestion Control," in *GLOBECOM 2024 - 2024 IEEE Global Communications Conference*, 2024, pp. 3805–3810.

[16] G. Sarkis, D. Vassilovski, A. F. Hanif, T. V. Nguyen, H. Cheng, S. Wu, S. Patil, and G. Marsh, "Considerations for Distributed Deployment of 5G NR V2X," in *2024 IEEE 100th Vehicular Technology Conference (VTC2024-Fall)*, 2024, pp. 1–6.

[17] T. Jiawei, C. J. Pawase, and K. Chang, "Adaptive Sidelink Open Loop Power Control Optimization Strategies for Vehicle-to- Vehicle Communications in 5G-NR-V2X," *IEEE Access*, vol. 12, pp. 25 079–25 089, 2024.

[18] Q. Fu, J. Liu, J. Wang, and J. Kong, "Toward Throughput Optimization: A Congestion Control Scheme for CAM Delivery via NR Sidelink," *IEEE Internet of Things Journal*, vol. 12, no. 9, pp. 12 206–12 218, 2025.

[19] H. Lee, C. Kim, E. Yang, and H. Kim, "Distributed Joint Congestion Control for V2X Using Multi-Agent Reinforcement Learning," in *2024 IEEE International Conference on Machine Learning for Communication and Networking (ICMLCN)*, 2024, pp. 268–273.

[20] Y. Wang, H. Gao, Z. Xiang, Y. Wang, and W. Wei, "Dynamic Graph-Based Deep Reinforcement Learning to V2X Channel Congestion Collaborative Control," *IEEE Transactions on Intelligent Transportation Systems*, pp. 1–18, 2025.

[21] Z. Chen, N. Pappas, E. Björnson, and E. G. Larsson, "Optimizing Information Freshness in a Multiple Access Channel With Heterogeneous Devices," *IEEE Open Journal of the Communications Society*, vol. 2, pp. 456–470, 2021.

[22] A. Baiocchi, I. Turcanu, N. Lyamin, K. Sjoöberg, and A. Vinel, "Age of Information in IEEE 802.11p," in *17th IFIP/IEEE International Symposium on Integrated Network Management (IM): ITAVT Workshop*. Virtual Conference: IEEE, 05 2021, pp. 1024–1031.

[23] J. Thunberg, D. Bischoff, F. A. Schiegg, T. Meuser, and A. Vinel, "Unreliable V2X Communication in Cooperative Driving: Safety Times for Emergency Braking," *IEEE Access*, vol. 9, pp. 148 024–148 036, 2021.

[24] I. Turcanu, A. Baiocchi, N. Lyamin, and A. Vinel, "An Age-Of-Information Perspective on Decentralized Congestion Control in Vehicular Networks," in *19th Mediterranean Communication and Computer Networking Conference (MedComNet)*. IEEE, 06 2021, pp. 1–8.

[25] M. M. Saad, M. A. Tariq, J. Seo, M. Ajmal, and D. Kim, "Age-of-information aware intelligent MAC for congestion control in NR-V2X," in *Fourteenth International Conference on Ubiquitous and Future Networks (ICUFN)*. IEEE, 2023, pp. 265–270.

[26] A. Dayal, V. K. Shah, H. S. Dhillon, and J. H. Reed, "Adaptive RRI Selection Algorithms for Improved Cooperative Awareness in Decentralized NR-V2X," *IEEE Access*, vol. 11, pp. 134 575–134 588, 2023.

[27] A. Rolich, I. Turcanu, and A. Baiocchi, "AoI-Aware and Persistence-Driven Congestion Control in 5G NR - V2X Sidelink Communications," in *2024 22nd Mediterranean Communication and Computer Networking Conference (MedComNet)*, 2024, pp. 1–4.

[28] P. A. Lopez, M. Behrisch, L. Bieker-Walz, J. Erdmann, Y.-P. Flötteröd, R. Hilbrich, L. Lücken, J. Rummel, P. Wagner, and E. Wiessner, "Microscopic traffic simulation using sumo," in *2018 21st International Conference on Intelligent Transportation Systems (ITSC)*, 2018, pp. 2575–2582.

[29] 3GPP, "NR; Medium Access Control (MAC) protocol specification (Release 18)," TS 38.321 V18.6.0, 06 2025.

[30] ——, "NR; Radio Resource Control (RRC) protocol specification (Release 18)," TS 38.331 V18.6.0, 06 2025.

[31] R. Iwaki, J. Nakazato, K. Maruta, M. Tsukada, H. Ochiai, and H. Esaki, "Enhancing V2X Communication: Machine Learning Assisted Dynamic mmWave Beam Search," in *2024 Fifteenth International Conference on Ubiquitous and Future Networks (ICUFN)*, 2024, pp. 404–409.

[32] 3GPP, "Study on evaluation methodology of new Vehicle-to-Everything (V2X) services (Release 15)," TR 37.885, 6 2019.

[33] L. Lusvarghi, B. Coll-Perales, J. Gozalvez, and M. L. Merani, "Link Level Analysis of NR V2X Sidelink Communications," *IEEE Internet of Things Journal*, vol. 11, no. 17, pp. 28 385–28 397, 2024.

[34] 5G Automotive Association (5GAA), "C-V2X Use Cases and Service Level Requirements," Technical Report, 10 2017.

Authorized licensed use limited to: Universita degli Studi di Roma La Sapienza. Downloaded on October 27,2026 at 15:13:50 UTC from IEEE Xplore. Restrictions apply.